IEEE Access
Multidisciplinary | Rapid Review | Open Access Journal

Received July 1, 2019, accepted July 18, 2019, date of publication July 25, 2019, date of current version August 7, 2019.

Digital Object Identifier 10.1109/ACCESS.2019.2931083

A Novel Fault Tolerant Machine With Integral Slot Non-Overlapping Concentrated Winding

FENG CHAI, (Member, IEEE), LINA GENG, AND YULONG PEI
School of Electrical Engineering and Automation, Harbin Institute of Technology, Harbin 150001, China

Corresponding author: Yulong Pei (peiyulong1@163.com)

This work was supported by the National Natural Science Foundation of China under Grant 51677039.

ABSTRACT A novel fault tolerant machine with integral slot non-overlapping concentrated winding (ISNCW) is proposed in this paper. With the distribution of phase windings in axial, the proposed machine realized excellent isolation capability between different phases. The performance comparisons between the proposed machine and the traditional integer slot overlapping winding (ISOW) machine are made by the analytical method and finite element analysis (FEA). Compared to the ISOW machine, the proposed machine has better performance in low speed high torque applications, and much better fault tolerant capability and flux weakening capability. Especially, the proposed machine appears excellent performance in limiting the short circuit current and preventing the irreversible demagnetization of permanent magnet under short-circuit fault. The phase independent structure makes the maintenance and replacement of the fault module convenient and saves the maintenance cost further.

INDEX TERMS Concentrated winding, fault tolerant, integer slot, non-overlapping, permanent magnet, synchronous, windings.

I. INTRODUCTION

Electrical machine as the key part of the modern electric drive systems is facing more and more demands. The reliability and fault tolerant capability are especially important for permanent magnet synchronous machine (PMSM) applied in safety-critical applications, such as the electrical vehicle, more-electric aircraft, electrical ship propulsion, railway traction, wind power generation, etc. [1], [2].

The single layer fractional slot concentrated winding (FSCW) is most widely used in fault tolerant PMSMs due to good electrical, magnetic, thermal, and physical isolations between different phases [3], [4]. With the advent of FSCW, the modular design concept has been applied to the design of FSCW PMSM, in which the stator core is divided into multiple independent modules. In case of fault happened to one module, the replacement of fault module is convenient, the maintenance costs is reduced largely.[5]

A small slot opening width is usually selected to obtain a large inductance, thus reducing the short circuit current [6]. Also, the single layer FSCW permanent magnet fault tolerant machine has a good flux weakening capability and can run in a wide speed region due to the large inductance [7], [8]. But there are large amount of magnetomotive force (MMF) space harmonic in single layer FSCW, which will increase rotor losses, vibration and noise [9], [10]. Although many harmonic suppression methods are proposed [11]–[19], these methods lead to some drawbacks such as, the manufacture advantages of FSCW machines disappeared, and the inter-phase coupling increased due to the disappeared isolation between different phases. These drawbacks largely decreased the fault tolerant capability.

ISOW contains low magnetomotive force (MMF) space harmonic contents, but its overlapped end winding results in stronger coupling between different phases. And there are limited short-circuit current suppression capability due to the small winding inductance. At the same time, the overlapped winding makes the modular processing of the ISOW machine impossible. Thus, ISOW machine appears no fault tolerance.

To make up the shortages and utilize the advantages of ISOW machine, a novel fault tolerant machine with ISNCW is proposed in this paper. The topology of proposed fault tolerant ISNCW machine is presented in section II. In section III, the performance difference between the proposed ISNCW machine and the traditional ISOW machine with the same pole slot combination is analyzed by analytical method. The electromagnetic performance comparisons between the proposed ISNCW machine and ISOW machine made by 2D FEA are shown in section IV. Finally, conclusions are drawn in Section V

The associate editor coordinating the review of this manuscript and approving it for publication was Bora Onat.

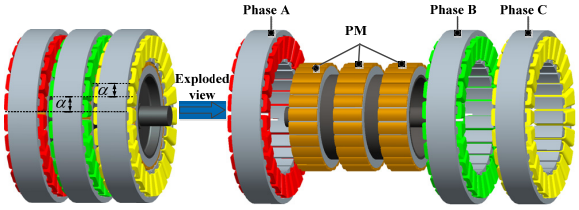

FIGURE 1. Structure of proposed ISNCW machines.

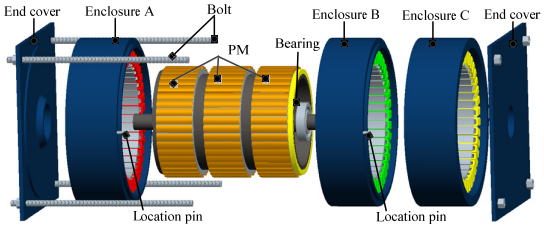

FIGURE 2. Exploded view of the prototype.

II. TOPOLOGY OF THE PROPOSED FAULT TOLERANT MACHINE

Figure 1 shows the topology of proposed fault tolerant ISNCW machine. The proposed machine has isolated phase windings to realize electrical, magnetic, thermal and physical isolation between different phases inherently. As shown in Figure 1, three-phase windings distribute along the axial direction and three phases have 120° electrical angle difference in circumferential direction. The corresponding mechanical angle difference α is $120°/p$ where p is pole pairs. The number of slots per phase is equal to the number of poles, namely the number of slots per pole per phase q is 1. Also, it can be seen that the three-phase rotors have no electrical angle difference.

As shown in Figure 1, the proposed machine is the modular design of phase-stator. Moreover, the modular design concept of stator-teeth can also be applied to the proposed machine, which can increase the slot fill factor and further improve the torque density.

Also, each phase can be further divided into multiple segregated single-phase winding sets in circumferential direction. The three-phase redundant winding drives can be applied in the proposed machine to realize better fault tolerant capability. Alternatively, the multi-phase winding drives can also be applied by increasing the number of phases in axial direction. The multi-phase winding drives are more applicable to slender-type structure due to the axial distribution of phase windings.

Figure 2 shows the exploded view of the prototype. It can be seen from Figure 2 that the enclosures are segmented too. The phase-stator and the enclosure are composed of one module. Therefore the maintenance and replacement of faulty phase are convenient, which saves maintenance costs and reduces the maintenance intervals.

III. THEORETICAL ANALYSIS

The goal of this section is to present the main difference between the proposed ISNCW machine and the traditional ISOW machine with the same pole slot combination based on some established analytical techniques.

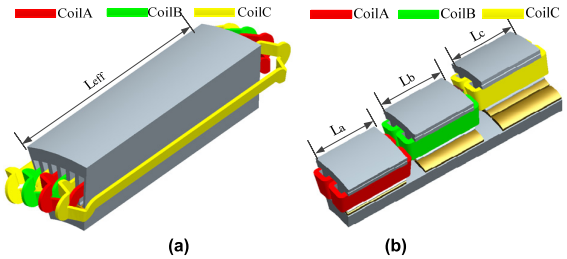

FIGURE 3. Machine structures (a) ISOW machine. (b) Proposed ISNCW machine.

A. INDUCTANCE

Figure 3 shows partial structure of ISOW machine and proposed ISNCW machine with the same pole slot combination.

From Figure 3, we can see that the proposed machine has three segments with equal length. The axial stack length of each segment is one third that of traditional ISOW machine. Namely, $L_a = L_b = L_c = L_{eff}/3$. There is only one phase winding in each stator cross section in the proposed machine. Although the slot number of two machines is the same, the tooth width and slot area of the proposed machine are triple that of ISOW machine.

Through the winding functions, the inductance calculation equation for surface-mounted permanent magnet (SPM) machines is expressed as follows.

$$L_{aa} = \frac{\mu_0 r_g L_{ef}}{g} \int_0^{2\pi} N_a^2(\theta) d\theta \tag{1}$$

$$L_{ab} = \frac{\mu_0 r_g L_{ef}}{g} \int_0^{2\pi} N_a(\theta) N_b(\theta) d\theta \tag{2}$$

$$L_{ad} = L_{aa} + L_{ab} \tag{3}$$

where L_{aa} is self-inductance of phase A, L_{ab} is mutual-inductance between phase A and B, L_{ad} is d-axis armature reaction inductance, L_{ef} is the active length per phase, μ_0 is the magnetic permeability of free space,r_g is average radius of air-gap,g is the effective air-gap length, θ is the position in the stator reference frame measured from the axis of phase A.

The winding function of the proposed machine under p pole pairs is shown in Figure 4. The self-inductance, mutual-inductance and d-axis armature reaction inductance of the traditional ISOW machine are calculated by equations (1)-(3) and shown in equation (4) (5) and (6).

$$L_{aa} = 2\pi \frac{\mu_0 r_g l_{eff}}{g} N_c^2 \tag{4}$$

$$L_{ab} = \frac{L_{aa}}{3} \tag{5}$$

$$L_{ad} = \frac{8\pi}{3} \frac{\mu_0 r_g l_{eff}}{g} N_c^2 \tag{6}$$

where N_c are the number of turns per coil for ISOW machine.

For the proposed ISNCW machine, the self-inductance of the proposed machine is derived by equation (1). Because the

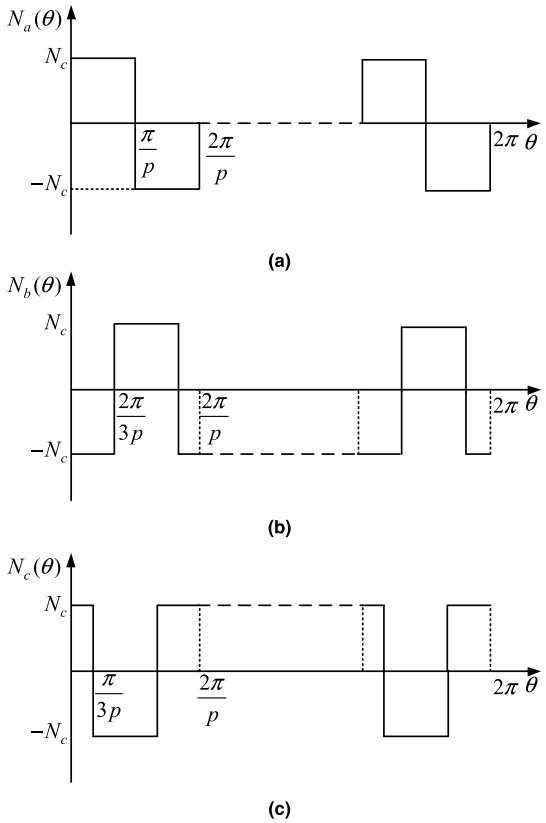

FIGURE 4. The winding function of phase A, B and C. (a) Phase A. (b) Phase B. (C) Phase C.

three phase-stators of the proposed machine is in different plane, thus the mutual-inductance is negligible. The mutual-inductance of the proposed machine is zero. The d-axis armature reaction inductance of the proposed machine is derived by equation (3). The self-inductance, mutual-inductance and d-axis armature reaction inductance of the proposed machine is shown in equation (7) (8) and (9).

$$L_{aa1} = 2\pi N_{c1}^2 \frac{\mu_0 r_g l_a}{g} \tag{7}$$

$$L_{ab1} = 0 \tag{8}$$

$$L_{ad1} = 2\pi \frac{\mu_0 r_g l_a}{g} N_{c1}^2 \tag{9}$$

where N_{c1} are the number of turns per coil for ISNCW machine respectively and $N_{c1} = 3N_c$.

The self-inductance and d-axis armature reaction inductance of the two machines have the following relationships:

$$\begin{cases} L_{aa1} = 3L_{aa} \\ L_{ad1} = 2.25L_{ad} \end{cases} \tag{10}$$

From the analysis above, we can see that the proposed machine has much larger self-inductance and d-axis armature reaction inductance than those of ISOW machine. Also, the mutual-inductance of proposed machines is zero, which can limit fault spread produced by the magnetically coupled theory. The aforementioned advantages provide optimized flux weakening performance and fault tolerant capability.

B. WORKING PRINCIPLE

The stator MMF per phase is pulsatile and can be expressed as follows.

$$F_A(\theta, t) = \sum_{v=2k\pm1} F_v \cos v\theta \cos \omega t \tag{11}$$

$$F_B(\theta, t) = \sum_{v=2k\pm1} F_v \cos\left[v(\theta - 120°)\right] \cos(\omega t - 120°) \tag{12}$$

$$F_C(\theta, t) = \sum_{v=2k\pm1} F_v \cos\left[v(\theta + 120°)\right] \cos(\omega t + 120°) \tag{13}$$

where v is the harmonic order and $k = 1, 2, 3 \ldots$, F_v is the amplitude of vth stator MMF harmonic. F_v is expressed as follows.

$$F_v = 0.9 \frac{1}{v} \frac{N_s k_{wv}}{p} I_1 \tag{14}$$

The synthesis of the three phase stators MMF of ISOW machine is a rotating MMF which can be written as follows.

$$F_s(\theta, t) = \sum_{v=6k\pm1} \frac{3}{2} F_v \cos(v\theta \pm \omega t) \tag{15}$$

whereas, the three phase stator MMF of the proposed machine cannot be synthesized to a rotating MMF due to the fact that the three phase windings are not in the same space. Therefore, the resultant torque of the whole machine is synthesized by torque produced by three phase units. Using analytical method in literature [20], the resultant torque is calculated by the following equation (16)-(27).

The rotor MMF harmonics are expressed as follows.

$$F_r(\theta, t) = \sum_{v=2k\pm1} F_{rv} \cos(v\theta - v\omega t - \varphi_v) \tag{16}$$

where φ_v is the phase angle difference between stator and rotor vth harmonic, F_{rv} is the amplitude of vth rotor MMF harmonic which is mainly decided by coercive force H_c and the thickness of the permanent.

When $v = 6k \pm 1$, $k = 0, 1, 2 \ldots$, torque produced by phase A, B and C are calculated as

$$T_{Av} = \frac{1}{2} vKF_v F_{rv} \begin{Bmatrix} \sin[(v \mp 1)\omega t + \varphi_v] \\ + \sin[(v \pm 1)\omega t + \varphi_v] \end{Bmatrix} \tag{17}$$

$$T_{Bv} = \frac{1}{2} vKF_v F_{rv} \begin{Bmatrix} \sin[(v \mp 1)\omega t + \varphi_v] \\ + \sin[(v \pm 1)\omega t + \varphi_v \mp 240°] \end{Bmatrix} \tag{18}$$

$$T_{Cv} = \frac{1}{2} vKF_v F_{rv} \begin{Bmatrix} \sin[(v \mp 1)\omega t + \varphi_v] \\ + \sin[(v \pm 1)\omega t + \varphi_v \pm 240°] \end{Bmatrix} \tag{19}$$

$$K = \frac{\mu_0 \pi r_g l_a}{2g} \tag{20}$$

The resultant torque of the machine produced by $(6k\pm1)$th order stator and rotor MMF harmonics is expressed as follows.

$$T_v = T_{Av} + T_{Bv} + T_{Cv} = \frac{3}{2} vKF_v F_{rv} \sin[(v \mp 1)\omega t + \varphi_v] \tag{21}$$

TABLE 1. The design specifications.

Specifications	Values
Rated power (kW)	48
Rated speed(rpm)	350
Rated current(A)	92
Rated torque(Nm)	1300
Amplitude of DC bus voltage(V)	650
Stator outer diameter(mm)	380

where μ_0 is permeability of air (H/m), g is the air-gap length (mm).

When $v = 3k, k = 1, 2\ldots$, torque produced by phase A, B and C is calculated respectively.

$$T_{Av} = \frac{1}{2}vKF_vF_{rv}\left\{\begin{array}{l}\sin\left[(v-1)\omega t+\varphi_v\right]\\+\sin\left[(v+1)\omega t+\varphi_v\right]\end{array}\right\} \quad (22)$$

$$T_{Bv} = \frac{1}{2}vKF_vF_{rv}\left\{\begin{array}{l}\sin\left[(v-1)\omega t+\varphi_v+120°\right]\\+\sin\left[(v+1)\omega t+\varphi_v-120°\right]\end{array}\right\} \quad (23)$$

$$T_{Cv} = \frac{1}{2}vKF_vF_{rv}\left\{\begin{array}{l}\sin\left[(v-1)\omega t+\varphi_v-120°\right]\\+\sin\left[(v+1)\omega t+\varphi_v+120°\right]\end{array}\right\} \quad (24)$$

The resultant torque produced by $3k$th stator and rotor MMF harmonic is obtained as follows.

$$T_v = T_{Av} + T_{Bv} + T_{Cv} = 0 \quad (25)$$

From the analysis above, only $(6k \pm 1)$th harmonics can produce torque, which is the same as traditional machines. For machine when pole pairs are p, the resultant torque of the proposed machine is expressed as

$$T(\theta, t) = \sum_{v=6k\pm1}\frac{3}{2}vpKF_vF_{rv}\sin\left[(v\mp1)\omega t+\varphi_v\right] \quad (26)$$

When $v = 1$, the constant torque is achieved as follows

$$T = \frac{3}{2}pKF_1F_{r1}\sin\varphi_1 \quad (27)$$

From the equation (27), we can see that the torque expression of the proposed ISNCW machine is the same as that of ISOW machine.

IV. MACHINE DESIGN

In order to compare the difference between the proposed ISNCW machine and traditional ISOW machine, two machines have been designed based on the design specifications in table 1. The stator and rotor cores are material 35WW250. The magnet is N40UH whose remanence is 1.285T. And the knee point of N40UH is 0.4T at 150°C.

It should be noted that the design principle of the proposed ISNCW machine is different from that of traditional ISOW machine due to different structures. The most obvious difference is the selection of pole slot combination. The proposed ISNCW machine has three phase segments, thus the axial length and phase resistance are increased. The concentrated winding combined with large number of poles is benefit in reducing the axial length, phase resistance and thickness of stator and rotor yoke [21], [22]. A relative high number of poles are advisable in the design of the proposed ISNCW machine to achieve high torque density and efficiency. Whereas the traditional ISOW machine is unsuitable to adopt such high number of poles like the proposed ISNCW machine does, which is because the tooth width of the traditional ISOW machine is very small when the number of poles is high. For fair comparison, two machines are constraint with the same stator outer diameter, slot opening width and effective axial stack length, and optimized respectively based on their own characteristics.

TABLE 2. Main parameters of two machines.

Items	ISNCW	ISOW
Number of poles	40	8
Number of slots	120	48
Stator inner diameter D_{i1} (mm)	280	254
Rotor inner diameter D_{i2} (mm)	240	180
Thickness of PM h_m (mm)	6	8
The slot pitch	1	5
Back iron thickness h_j (mm)	10.6	20.0
Tooth width T_w (mm)	12	9
Air-gap length g (mm)	1	1
Active stator stack length L (mm)	280	280
Number of turn in series N	270	96
Slot filling factors (%)	60	60
PM weight m_p (kg)	9.9	11.3
Total weight m_{all} (kg)	136.2	181.5

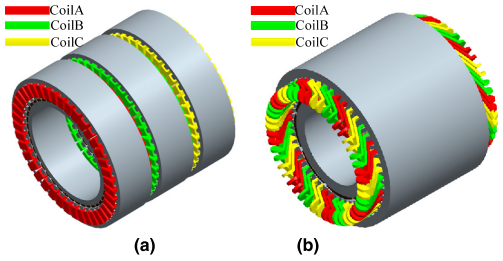

FIGURE 5. Machine structures. (a) Proposed ISNCW machine (b) ISOW machine.

Surface mounted permanent magnet (SPM) which has the advantages such as high efficiency, high torque density, simple structure, low manufacture cost and easy to optimize air gap flux density waveforms is adopted in this paper. And the eccentric pole is used to optimize the torque ripple.

The structure parameters of two machines with fixed stator outer diameter and active stator stack length are listed in table 2 and compared in Figure 5. The detailed comparison is made in the following sections.

V. PERFORMANCE COMPARISONS

In this section, performance comparisons between the proposed ISNCW machine and ISOW machine are made by 3-D FEA.

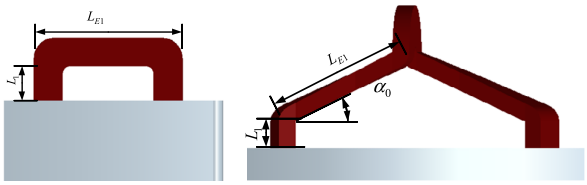

FIGURE 6. The 3-D model of end windings (a) ISNCW machine (b) ISOW machine.

TABLE 3. The axial length and phase resistance of two machines.

Items	ISNCW	ISOW
L_1 (mm)	5	10
L_E (mm)	70	25
α_0	0	30
L_{all} (mm)	360	376
R (Ω)	0.143	0.174

A. TOTAL AXIAL LENGTH AND PHASE RESISTANCE

Figure 6 shows the 3-D model of end windings for two machines, which is used to calculate the total axial length and phase resistance of two machines. The total axial length L_{all} and phase resistance is shown in table 3. It should be noted that the interval length between adjacent phases is 5mm, in which the mutual inductance between different phases is negligible.

It is seen that the total axial length and phase resistance of the proposed ISNCW machine is smaller than that of ISOW machine.

B. HEALTHY OPERATION PERFORMANCE

The simulation results shown in this section are based on the parameters listed in table 2 at rated speed 350rpm. The proposed ISNCW machine has larger fundamental winding factor and stator inner diameter than those of ISOW machine, which results in higher amplitude of back EMF. The fundamental winding factor of the proposed machine and ISOW machine is 1 and 0.933 respectively. Figure 7 and Figure 8 show the waveform of open-circuit air-gap flux density and back EMF and the corresponding fast Fourier transformation (FFT). As shown in Figure 7, the fundamental amplitude of the air-gap flux density of the proposed ISNCW machine is lower than that of ISOW machine. But, we can see from Figure 8 that the fundamental amplitude of back EMF of the proposed ISNCW machine is larger than that of ISOW machine.

Table 4 shows the Total Harmonics Distortion (THD) of the air-gap flux density and phase back EMF. From table 4 we can see that the THD of air-gap flux density and phase back EMF of the proposed ISNCW machine is lower than that of ISOW machine.

Figure 9 compares electromagnetic toque and the corresponding FFT of two machines. We can see from

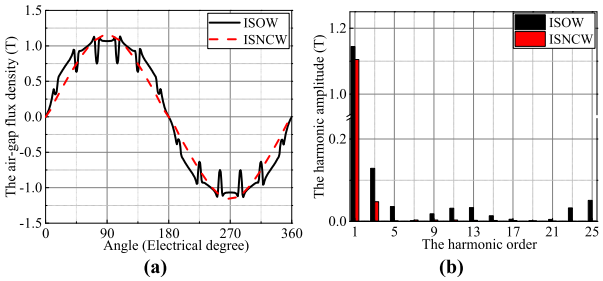

FIGURE 7. The air-gap flux density (a) Waveforms (b) The FFT of the air-gap flux density.

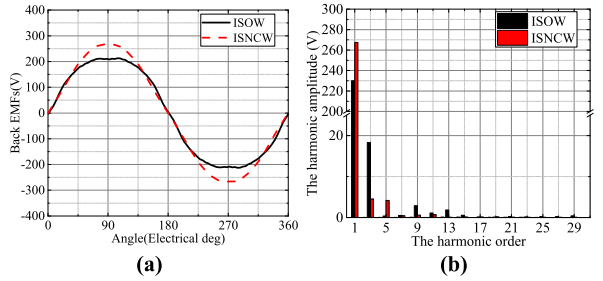

FIGURE 8. The phase back EMF (a) Waveforms (b) The FFT of back EMF.

TABLE 4. The THD of air-gap flux density and phase back EMF.

Items	ISNCW	ISOW
THD of air-gap flux density(%)	5.1	13.6
THD of phase back EMF(%)	2.3	8.1

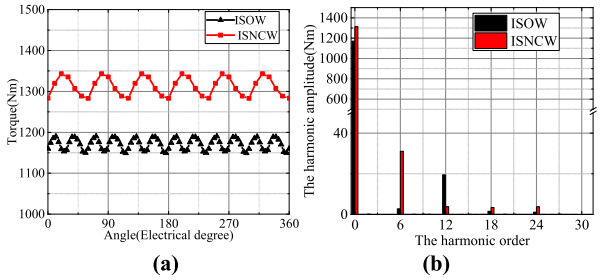

FIGURE 9. The electromagnetic torque (a) Waveforms (b) The FFT of electromagnetic torque.

Figure 9 that the proposed ISNCW machine has higher average electromagnetic torque compared to ISOW machine. It is because that the proposed machine has higher fundamental harmonic amplitude of back EMFs than that of ISOW machine.

Since slots per pole per phase of the proposed ISNCW machine is 1, thus the harmonic torque ripple of the proposed ISNCW machine is slightly higher than that of ISOW machine.

The analysis above proved the validity of proposed machine.

The 3d and 2d distribution of flux density is shown in Figure 10. We can see that the flux density of the proposed

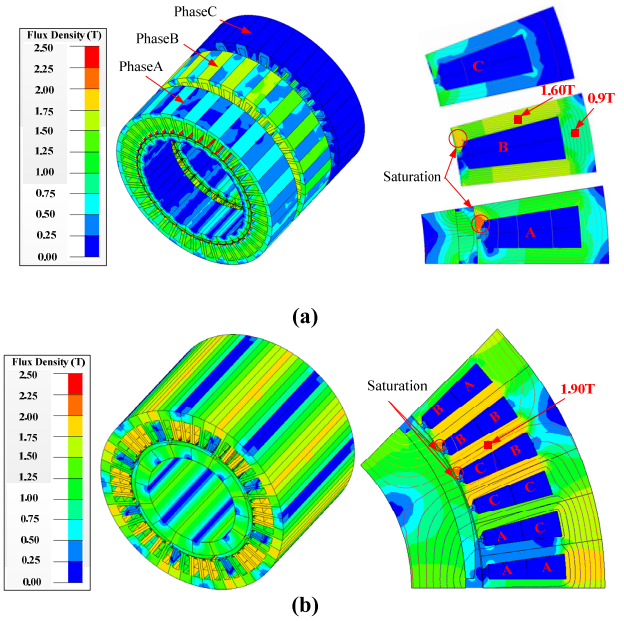

FIGURE 10. Distribution of flux density (a)ISNCW machine (b)ISOW machine.

machine at stator yoke and tooth is much lower than that of ISOW machine.

For traditional ISOW machine, there are six teeth under one pole of ISOW machine. As is shown in Figure 10 (b), flux lines mainly concentrate on four teeth. For the proposed ISNCW machine, there is only one tooth under one pole of ISNCW machine. As is shown in Figure 10 (a), the flux lines have to pass through this tooth. If the number of poles of the proposed ISNCW machine is the same to that of the traditional ISOW machine, the tooth width of the proposed ISNCW machine is equal to the total width of six teeth of the traditional ISOW machine. Therefore the flux density of the proposed machine on stator tooth is smaller than that of ISOW machine. Because rotor is rotated, thus the distribution of flux density is changed with rotor position. At the position in Figure 10 (a) the flux line is concentrated in tooth tip of phase A, thus the proposed ISNCW machine is saturate at stator tooth tip of phase A.

Also, the number of poles of the proposed machine is much larger than that of ISOW machine, thus the flux density of the proposed machine on stator yoke is lower than that of ISOW machine.

The torque density, losses and efficiency of the two machines at rated speed are calculated and listed in table 5. It is obviously that the proposed ISNCW machine has higher torque density and efficiency than that of ISOW machine. Because that the proposed machine has thinner stator and rotor back iron and higher fundamental harmonic winding factor compared to traditional ISOW machine, thus the torque density of the proposed machine is higher. Compared to core loss and PM eddy current loss, copper loss is the main source of loss at low speed, thus the efficiency of the proposed machine is higher than that of ISOW machine.

TABLE 5. FEA results.

Items	ISNCW	ISOW
Torque (Nm)	1312	1171
Torque density (Nm/kg)	9.6	6.5
Iron loss (W)	283	107
PM eddy current loss (W)	49	13
Copper loss (W)	3631	4418
Efficiency (%)	92.4	90.4
Power factor	0.84	0.94
Torque ripple(%)	2.28	1.74

The power factor of the proposed ISNCW machine is lower than that of ISOW machine due to the fact that the proposed machine has higher reactance than that of ISOW machine which is proved in the following section. But all fault tolerant PM machines with high short-circuit current reduction capability have large reactance and hence low power factor.

The most obvious difference of two machines is the number of poles. The proposed ISNCW machine adopts high number of poles to achieve high torque density. Thus proposed ISNCW machine is suitable to low speed and high torque applications in consideration of the larger rotor loss in high speed. The traditional ISOW machine which has much lower number of poles than that of ISNCW machine is suitable for relatively high speed applications. The proposed ISNCW machine has better performance than that of ISOW machine in low speed and high torque fields and makes up the application of integer slot winding in low speed and high torque fields.

C. SHORT-CIRCUIT FAULT PERFORMANCE

A fault tolerant machine must have better electrical, magnetic, thermal and physical isolation to limit the spread of faults between different phases. As described in section II, the proposed ISNCW machine inherently has better electrical, magnetic, thermal and physical isolation between different phases.

Compared to open circuit fault, short circuit fault is more dangerous. The big short circuit current will cause large copper loss which damages the insulation and causes the irreversible demagnetization of permanent magnet. In the case of short circuit failure occurs in an inverter switch or in one phase winding, a terminal short circuit is usually applied by closing all the bottom or top switches of the inverter [23]–[25]. Thus, this paper mainly investigated the three-phase symmetrical short-circuit fault.

In the case of three-phase symmetrical short circuit fault, the amplitude of the steady short circuit current is as follows [24], [26].

$$I_{dsc} = -\frac{\omega_r^2 L_q \psi_f}{R^2 + \omega_r^2 L_d L_q} \tag{28}$$

$$I_{qsc} = -\frac{\omega_r R \psi_f}{R^2 + \omega_r^2 L_d L_q} \tag{29}$$

where ψ_f is the permanent magnet flux linkage, ω_r is electrical angular speed, L_d and L_q is d-axis and q-axis inductance.

TABLE 6. The inductance, flux linkage and characteristic current.

	ψ_f (Wb)	L_{aa} (mH)	L_{ab} (mH)	L_d (mH)	C_f (%)	I_{ch} (A)
ISNCW	0.36	3.17	0	3.17	0	113.56
ISOW	1.61	4.84	1.57	6.41	32.43	251.17

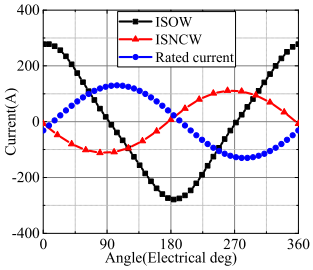

FIGURE 11. Three-phase symmetrical steady-state short-circuit current and rated current.

At high speed, the resistance R is neglected. Thus the steady short circuit current is equal to the characteristic current I_{ch}, as shown in equation (30).

$$I_{ch} = -\frac{\psi_f}{L_d} \tag{30}$$

Therefore, the amplitude of steady short circuit current is decreased as the amplitude of d-axis inductance increases.

The permanent magnet flux linkage ψ_f, inductance and the calculated characteristic current I_{ch}, are listed in table 6. It should be noted that the mutual-inductance of the proposed ISNCW machine is calculated by 3D FEA, which is very close to zero. In order to save calculation time, the results listed in table 5 are all calculated by 3-D FEA.

It can be seen that the coupling coefficient C_f (the ratio of the mutual-inductance to the self-inductance) of ISOW machine and ISNCW machine is 32.43% and 0% respectively, which proves better isolation performance between different phases in the proposed ISNCW machine. And the characteristic current of proposed ISNCW machine is much lower than that of ISOW machine, which indicates smaller short circuit current of the proposed ISNCW machine.

Figure 11 shows the three-phase symmetrical steady state short circuit currents calculated by FEA. It is proved that the steady-state short-circuit current of the proposed ISNCW machine is very close to the rated current and much lower than that of ISOW machine. Such low short-circuit current is achieved inherently in the proposed machine.

Figure 12 shows the flux density distribution of the PM under three-phase symmetrical short-circuit fault. We can see that the minimum flux density of the PM in the proposed ISNCW machine and ISOW machine is 0.60T and 0.27T respectively. And the irreversible demagnetization of PM will happen to the ISOW machine in which the flux density is lower than 0.4T when the temperature of the PM is higher than 150°C. It is because the demagnetization current and the copper loss of the proposed ISNCW machine is much lower than that of ISOW machine under short circuit fault.

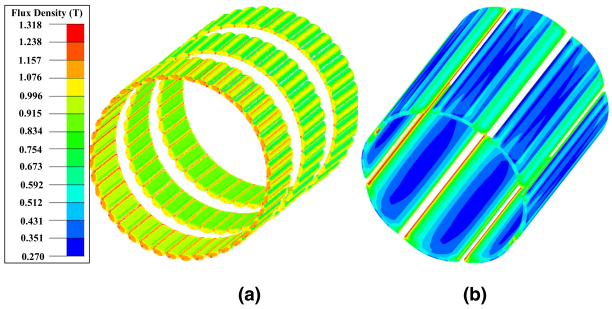

FIGURE 12. Flux density distributions of the PM under three-phase symmetrical short-circuit condition (a) ISNCW machine (b) ISOW machine.

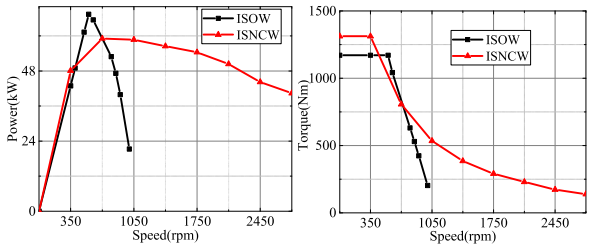

FIGURE 13. The flux weakening performance. (a) Power vs speed curves. (b) Torque vs speed curves.

D. FLUX WEAKENING CAPABILITY

As is stated in reference [8], to acquire an optimal flux weakening, the characteristic current is equal to the rated current. It is widely known that the inductance values of SPM machines are very low in ISOW machines due to the large effective air-gap length. Therefore, the characteristic current value for SPM machines is much higher than the rated current. It is difficult to decrease the permanent magnet flux linkage ψ_f in SPM machines without decreasing the machine's torque production capability. As a result, the flux weakening operation is limited by large characteristic current in SPM machines.

Through part C in this section, it is obvious that the proposed ISNCW machine has much lower characteristic current. Figure 13 shows the power curves and the torque curves under various speeds, respectively. It can be seen that the ratio of constant power speed region to constant torque speed region between the proposed ISNCW machine and ISOW machine is 5.28:1 and 0.55:1, respectively.

The lower characteristic current in proposed ISNCW machines results in wide constant power speed region. Thus, the proposed ISNCW machine has more optimal flux weakening capability compared to traditional ISOW machines. And the proposed SPM ISNCW machine has realized both low speed high torque and wide constant power speed region.

VI. CONCLUSION

In this paper, a novel fault tolerant machine with ISNCW is proposed. The performance comparison between the proposed machine and ISOW machine has been investigated by analytical method and FEA. The results are shown as follows:

1) The proposed machine inherently has better isolation capability between different phases.

2) The proposed machine has better performance than that of ISOW machines at low speed and high torque applications.

3) The proposed machine inherently has lower characteristic current to obtain some advantages such as a lower short circuit current, better fault tolerant capability and flux weakening performances.

4) The independent phase winding structure makes the maintenance and replacement of the fault module more convenient, which save the maintenance cost.

REFERENCES

[1] W. Zhao, L. Xu, and G. Liu, "Overview of permanent-magnet fault-tolerant machines: Topology and design," *CES Trans. Elect. Mach. Syst.*, vol. 2, no. 1, pp. 51–64, 2018.

[2] Y. Wang and W. Hao, "A torque impulse balance control for multi-tooth fault tolerant switched-flux machines under open-circuit fault," *Energies*, vol. 11, no. 7, p. 1919, 2018.

[3] D. Ishak, Z. Q. Zhu, and D. Howe, "Comparative study of permanent magnet brushless motors with all teeth and alternative teeth windings," in *Proc. 2nd Int. Conf. PEMD*, Edinburgh, U.K., Mar. 2004, pp. 834–839.

[4] N. Bianchi, M. D. Pré, G. Grezzani, and S. Bolognani, "Design considerations on fractional-slot fault-tolerant synchronous motors," in *Proc. IEEE IEMDC*, San Antonio, TX, USA, May 2005, pp. 902–909.

[5] P. Zheng, F. Wu, Y. Lei, Y. Sui, and B. Yu, "Investigation of a novel 24-slot/14-pole six-phase fault-tolerant modular permanent-magnet in-wheel motor for electric vehicles," *Energies*, vol. 6, no. 10, pp. 4980–5002, Sep. 2013.

[6] B. C. Mecrow, A. G. Jack, and J. A. Haylock, "Fault-tolerant permanent magnet machine drives," *IEE Proc. Electr. Power Appl.*, vol. 143, no. 6, pp. 433–437, 1996.

[7] W. Tian, H. Guo, and H. Qian, "Analysis and study of flux weakening performance in fault-tolerant permanent magnet machine," in *Proc. AUS-IEEE/CSAA Int. Conf. Aircr. Util. Syst.*, Beijing, China, Oct. 2016, pp. 1062–1066.

[8] A. M. El-Refaie and T. M. Jahns, "Optimal flux weakening in surface PM machines using fractional-slot concentrated windings," *IEEE Trans. Ind. Appl.*, vol. 41, no. 3, pp. 790–800, May/Jun. 2005.

[9] N. Bianchi, S. Bolognani, and P. Frare, "Design criteria for high-efficiency SPM synchronous motors," *IEEE Trans. Energy Convers.*, vol. 21, no. 2, pp. 396–404, Jun. 2006.

[10] A. M. El-Refaie, "Fractional-slot concentrated-windings synchronous permanent magnet machines: Opportunities and challenges," *IEEE Trans. Ind. Electron.*, vol. 57, no. 1, pp. 107–121, Jan. 2010.

[11] Y. Wang, R. Qu, and J. Li, "Multilayer windings effect on interior PM machines for EV applications," *IEEE Trans. Ind. Appl.*, vol. 51, no. 3, pp. 2208–2215, May/Jun. 2015.

[12] P. Reddy, A. M. El-Refaie, and K.-K. Huh, "Effect of number of layers on performance of fractional-slot concentrated-windings interior permanent magnet machines," *IEEE Trans. Power Electron.*, vol. 30, no. 4, pp. 2205–2218, Apr. 2015.

[13] P. B. Reddy, K. K. Huh, and E. L. R. Ayman, "Effect of stator shifting on harmonic cancellation and flux weakening performance of interior PM machines equipped with fractional-slot concentrated windings for hybrid traction applications," in *Proc. IEEE Energy Convers. Congr. Expo. (ECCE)*, Raleigh, NC, USA, Sep. 2012, pp. 525–533.

[14] P. B. Reddy, K.-K. Huh, and A. M. El-Refaie, "Generalized approach of stator shifting in interior permanent-magnet machines equipped with fractional-slot concentrated windings," *IEEE Trans. Ind. Electron.*, vol. 61, no. 9, pp. 5035–5046, Sep. 2014.

[15] G. Dajaku and D. Gerling, "A novel tooth concentrated winding with low space harmonic contents," in *Proc. IEEE Int. Electr. Mach. Drives Conf. (IEMDC)*, Chicago, IL, USA, May 2013, pp. 755–760.

[16] K. Wang, Z. Q. Zhu, G. Ombach, M. Koch, S. Zhang, and J. Xu, "Electromagnetic performance of an 18-slot/10-pole fractional-slot surface-mounted permanent-magnet machine," *IEEE Trans. Ind. Appl.*, vol. 50, no. 6, pp. 3685–3696, Nov./Dec. 2014.

[17] A. S. Abdel-Khalik, S. Ahmed, and A. M. Massoud, "Low space harmonics cancelation in double-layer fractional slot winding using dual multiphase winding," *IEEE Trans. Magn.*, vol. 51, no. 5, May 2015, Art. no. 8104710.

[18] A. S. Abdel-Khalik, S. Ahmed, and A. M. Massoud, "A six-phase 24-slot/10-pole permanent-magnet machine with low space harmonics for electric vehicle applications," *IEEE Trans. Magn.*, vol. 52, no. 6, Jun. 2016, Art. no. 8700110.

[19] A. S. Abdel-Khalik, S. Ahmed, and A. M. Massoud, "Effect of multilayer windings with different stator winding connections on interior PM machines for EV applications," *IEEE Trans. Magn.*, vol. 52, no. 2, Feb. 2016, Art. no. 8100807.

[20] A. M. El-Refaie, T. M. Jahns, and D. W. Novotny, "Analysis of surface permanent magnet machines with fractional-slot concentrated windings," *IEEE Trans. Energy Convers.*, vol. 21, no. 1, pp. 34–43, Mar. 2006.

[21] C. M. Spargo, B. C. Mecrow, and J. D. Widmer, "Higher pole number synchronous reluctance machines with fractional slot concentrated windings," in *Proc. 7th IET Int. Power Electr., Mach. Drives. Conf. (PEMD)*, Manchester, U.K., 2014, pp. 1–5.

[22] J. Pyrhönen, T. Jokinen, and V. Hrabovcová, *Design of Rotating Electrical Machines*. Hoboken, NJ, USA: Wiley, 2008.

[23] Y. Sui, P. Zheng, Z. Yin, M. Wang, and C. Wang, "Open-circuit fault-tolerant control of five-phase PM machine based on reconfiguring maximum round magnetomotive force," *IEEE Trans. Ind. Electron.*, vol. 66, no. 1, pp. 48–59, Apr. 2018.

[24] G. Choi and T. M. Jahns, "Interior permanent magnet synchronous machine rotor demagnetization characteristics under fault conditions," in *Proc. IEEE Energy Convers. Congr. Expos. (ECCE)*, Denver, CO, USA, Sep. 2013, pp. 2500–2507.

[25] G. Choi and T. M. Jahns, "Investigation of key factors influencing the response of permanent magnet synchronous machines to three-phase symmetrical short-circuit faults," *IEEE Trans. Energy Convers.*, vol. 31, no. 4, pp. 1488–1497, Jul. 2016.

[26] M. Barcaro, N. Bianchi, and F. Magnussen, "Six-phase supply feasibility using a PM fractional-slot dual winding machine," *IEEE Trans. Ind. Appl.*, vol. 47, no. 5, pp. 2042–2050, Sep./Oct. 2011.

FENG CHAI (M'13) received the B.E. degree in electrical engineering from Xi'an Jiaotong University, Xi'an, China, in 1994, and the M.E. and Ph.D. degrees in electrical engineering from the Harbin Institute of Technology, Harbin, China, in 1998 and 2003, respectively, where she is currently a Professor of electrical engineering.

She works on the design of permanent magnet machines and drives.

LINA GENG received the B.S. degree in electrical engineering from the Harbin University of Science and Technology (HUST), Harbin, China, in 2013, and the M.S. degree in electrical engineering from the Harbin Institute of Technology, Harbin, in 2015, where she is currently pursuing the Ph.D. degree with the School of Electrical Engineering and Automation.

Her current research interest includes permanent magnet synchronous machines.

YULONG PEI received the B.E., M.E., and Ph.D. degrees in electrical engineering from the Harbin Institute of Technology, Harbin, China, in 2002, 2004, and 2009, respectively, where he is currently an Associate Professor of electrical engineering.

His research interest includes the design of permanent magnet machine.